Nigerian Journal of Physics (NJP)
ISSN online: 3027-0936
ISSN print: 1595-0611
DOI: https://doi.org/10.62292/njp.v35i2.2026.472
Volume 35(2), June 2026

Studies of the Effect of Neodymium Nanoparticles on Radiation Shielding Properties of Zinc-Tellurite Glass System

***Abubakar Abba Aji, Aliyu Mohammed Aliyu, Dauda Abubakar, Abdulkadir Adamu, Alameen Mustapha Muhammed and Auwal Baballe**

Department of Physics, Sa'adu Zungur University, Bauchi State, Nigeria.

*Corresponding Author's Email: ajiabbaabubakar002@gmail.com Phone: +2348140852019

ABSTRACT

The study seeks to evaluate the radiation shielding properties of Neodymium Nanoparticles doped Zinc-Tellurite Glass System with chemical composition $[(TeO_2)_{0.70}(ZnO)_{0.30}]_{(1-x)}(Nd_2O_3\ NPs)_{(x)}$, x = 0.01, 0.02, 0.03,0.04, and 0.05 mol glass, and are coded as S1, S2, S3, S4 and S5 in increasing Nd_2O_3. The glasses were prepared by using a conventional method of melt quenching. Phy-X/PSD simulation software was used to determine the mass attenuation coefficient (MAC), linear attenuation coefficient (LAC), half value layer (HVL), effective atomic number (Zeff) of the investigated glasses. The maximum values for all the glasses were observed at the lowest tested energy, 0.28 MeV. At this energy, the MAC of the glasses can be observed to increase as the Nd_2O_3 concentration of the sample increases as well, which could be due to the increase in density. The minimum HVL values occurred at the lowest tested energy, 0.2447 MeV, and increased with increasing energy, meaning that the glasses are more effective at lower energies. The results proved that the S5 glass, the glass with the greatest Nd_2O_3 content and density, has the greatest potential for radiation shielding applications.

Keywords: Neodymium, Radiation, Shielding, Zinc-Tellurite, Glass.

INTRODUCTION

Devices that generate artificial ionizing radiation, such as X-rays and γ-rays, have been widely adopted in a variety of industrial, medical, and nuclear configurations. This widespread adoption is a direct result of the utilization of technological breakthroughs. Nevertheless, prolonged and excessive exposure to such radiation can have adverse effects on health, potentially leading to the development of cancer, as well as symptoms such as vomiting, nausea, and, in severe situations, even mortality (Dong et al., 2021). The interaction of high-energy photons with human tissue results in the ionization of water molecules, leading to the formation of reactive free radicals. These radicals can induce significant biological damage, including both surface-level and internal disruption of DNA structure. Such damage may result in mutations, cell dysfunction, or cell death. In addition to photons, other forms of ionizing radiation such as neutrons, γ-rays, and X-rays also pose serious risks to humans, animals, and the environment due to their high penetration power and ionization capability. For these reasons, minimizing exposure to ionizing radiation is critical, and there is considerable research interest in the development of improved materials for radiation attenuation and shielding (Alajerami et al., 2020). To decrease the amount of hazardous radiation that workers are exposed to, it is well known that shielding and attenuation materials act as a barrier between the sources of radiation that release radiation and the surrounding area or the workers themselves. When it comes to minimizing or reducing the potentially harmful effects of radiation, one of the fundamental concepts of radiation protection is the selection of appropriate shielding materials. This is one part of the radiation protection process. This particular selection is of utmost significance. This specific aspect of the situation is still the subject of investigations and study inquiries that are currently being carried out. Polymers, natural rocks, rubber, concrete, brick, and alloy are just some of the materials that have been investigated in a number of studies that have been published in the literature (Singh et al., 2020).

For several years, lead and concrete were the best choice for shielding, despite the great benefits of metallic lead in terms of advanced attenuating characteristics in particular to the higher photon energies (i.e. gamma-

rays), the toxicity issue on humans and the environment has recently begun to be restricted its wide preference (Vani et al., 2021).

Generally, the actual shielding material depends on some factors, such as high density and atomic number, radiation resistance, ease with which heat dissipates, ability to lower levels of radiation, required thickness, permanence of shielding, possibilities of multi-use, and obtainability. Some scientists studied and tested different materials, including alloys, polymers, concrete, glass, and glass-ceramics for ionizing radiation shielding applications (Itas et al., 2024). Among all the aforementioned materials, glasses demonstrated superb shielding suitability owing to their ease of fabrication, transparency, and flexibility of design (Geidam et al., 2022).

Glasses were recently developed as novel appropriate gamma photon protection materials. Glasses options demonstrated remarkable shielding suitability, due to their optical transparency, cost-effectiveness, as well as environmental sustainability through recyclability and flexibility in shape and size. The formation of glass systems involves glass formers, intermediates and modifiers. The formers are Silicate SiO_2, Borate B_2O_3, Phosphate P_2O_5, Telluride TeO_2, and Germanite GeO_2 glasses. Glass formation require the addition of modifiers and intermediates to create a stable and durable glass system (Mahmoud et al., 2022).

Nowadays, focus on the fabrication of tellurite glasses cannot be overemphasized due to their notable features like high dielectric constant, index of refraction (, low phonon energy (~750 cm^{-1}), broad infrared transmittance, and low melting temperature. Besides the above-mentioned properties, they possess a high coefficient of thermal expansion and less hygroscope, contrary to phosphate and borate glasses (Dong et al., 2021). The incorporation metals, such as MgO, ZnO and BaO, into the glass system, substantially increases the shielding features of glass. Because Zinc has a high density and absorption cross section, it is said to have a high effectiveness of radiation attenuation. According to earlier studies, doping glass structures with rare earth (RE^{3+}) ions such as Eu^{3+}, Sm^{3+}, Nd^{3+}, and Dy^{3+} improves optical properties and raises density. Among Rare earth elements, Nd^{3+} is a promising option for solid-state lasing, solar energy, fiber optics and radiation protection (Sayyed, 2024).

By introducing nanoparticles into the composition of glass, the radiation shielding properties of glass can be enhanced, as well as its structural and mechanical properties. Nanoparticles improve these characteristics by improving the bulk properties or packing model structure of the glass samples. Much literature has been conducted to evaluate impact of particle size on the shielding ability of the samples greatly diminishes as energy increases, meaning that smaller particles perform better against lower energy photons (Halimah et al., 2019). The aim of this research is to evaluate radiation shielding properties of Neodymium Nanoparticles doped Zinc-Tellurite Glass System

MATERIALS AND METHODS

The radiation shielding properties of Neodymium Nanoparticles doped Zinc-Tellurite Glass System were determined using computational software Phy-X/PSD and XCOM. The parameters calculated include: Mass Attenuation Coefficient (MAC), Linear Attenuation Coefficient (LAC) Half-Value Layer (HVL) and Mean Free Path (MFP). These calculations help in evaluating the effectiveness of these glasses for radiation shielding applications.

Materials

The materials used in this research work include Phy-X/PSD software (version 3), a laptop computer (HP-2560) with a 64-bit operating system, 8.00 GB RAM, and Windows 10 installed, as well as Microsoft Office 2023.

Sample Preparation

The glass samples of Nd^{3+} doped zinc tellurite glass system with chemical formula $[(TeO_2)_{0.70}(ZnO)_{0.30}]_{(1-x)}(Nd_2O_3\ NPs)_{(x)}$, x = 0.01, 0.02, 0.03, 0.04, and 0.05 mol, were prepared by using a conventional method of melt quenching by (Halimah et al., 2020). High purity raw materials (99.99%, purity grade) of TeO_2 (Puratronic, Alfa Aesar), ZnO (Assay, Alfa Aesar), and Nd_2O_3 nanoparticles (Assay, AlfaAesar) were used to prepare the glass samples. The oxide components used in preparing the glasses were weighed by using a high accuracy (±0.0001g) digital weighing machine and mixed together in an alumina crucible. The mixture was put in a furnace for 1hour at 400 to allow complete drying of the mixture. After heating, the mixture was transferred to a second furnace at 830°C for 90 minutes for the melting process. The glass compositions and their respective densities are listed in Table 1.

Table 1: The Doped Chemical Composition $[(Teo_2)_{0.70}(Zno)_{0.30}]_{(1-x)}$ $(Nd_2O_3\ Nps)_{(X)}$, x = 0.01, 0.02, 0.03, 0.04, And 0.05 Mol

Glass Code	TeO_2	ZnO	Nd_2O_3 NPs	Density (g/cm^3)
S1	0.693	0.297	0.01	5.39
S2	0.686	0.294	0.02	5.44
S3	0.676	0.291	0.03	5.51
S4	0.672	0.288	0.04	5.57
S5	0.665	0.285	0.05	5.61

Radiation Shielding Simulation

The radiation shielding parameters of the Neodymium Nanoparticles doped Zinc-Tellurite Glass System were determined using user friendly online Phy-X/PSD software developed by (Sakar *et al*., 2020) and XCOM software. The shielding parameters were calculated in the energy range from 0.015 to 15 MeV.

Phy-X/PSD Software

Phy-X/PSD software, recently developed by Sakar et al. (2020) for evaluating radiation shielding parameters of various materials, was employed in this study. The calculation procedure begins with inputting the material's chemical composition and density into the program. Within the software, compositions can be defined in terms of mole fractions. The shielding parameters are then computed across a broad energy range by selecting appropriate energy sources (^{22}Na, ^{55}Fe, ^{60}Co, ^{109}Cd, ^{131}I, ^{133}Ba, ^{137}Cs, ^{152}Eu, ^{241}Am, as well as the K-shell energies of Cu, Rb, Mo, Ag, Ba, and Tb) (Sakar et al., 2020). Finally, the software determines the required

RESULTS AND DISCUSSION

A computational analysis using Phy-X/PSD software was carried out to assess the radiation shielding performance of Nd^{3+} doped zinc tellurite glass system. Theoretical evaluations provided several shielding parameters, including the Mass Attenuation Coefficient (MAC), Linear Attenuation Coefficient (LAC) Half-Value Layer (HVL) and Mean Free Path (MFP) and fast neutron removal cross section (ΣR) within the energy range of 0.015 to 15 MeV, originating from ^{137}Cs and ^{60}Co sources. Additionally, a comparative study was conducted to examine the shielding efficiency across different Nd^{3+} doped zinc tellurite glass system compositions.

Mass Attenuation (MAC)

The key factor in describing any material's gamma radiation absorption characteristics is the mass attenuation coefficient (MAC), with higher values indicating more effective gamma radiation shielding. Fig. 1 and Table 2 depict the variation of MAC (cm^2/g) with the gamma-ray photon energy (MeV) for the five analyzed glass systems. Consistent with prior studies on mass attenuation, our results also demonstrate that MAC values are higher at the lower photon energy of 15 KeV, increasing from 28.691 cm^2/g to 51.748 cm^2/g as the Nd_2O_3 concentration increases from 0.01 to 0.05 mol. The progressive rise in MAC from samples S1 to S5 suggests a dependence on the Nd_2O_3 content, or oxide ion concentration, possibly due to substituting heavier Nd_2O_3 molecules with lighter TeO_2 molecules in the glass system.

Table 2: MAC Values of the $[(Teo_2)_{0.70}(Zno)_{0.30}]_{(1-x)}$ $(Nd_2O_3\ Nps)_{(X)}$, x = 0.01, 0.02, 0.03, 0.04, And 0.05 Mol Glass System Obtained Using Phy-X/PSD Software

Energy (MeV)	Mass Attenuation Coefficient (cm^2/g)				
	S1	S2	S3	S4	S5
0.015	28.691	36.577	42.739	47.687	51.748
0.02	13.288	16.976	19.858	22.172	24.071
0.03	4.523	5.771	6.746	7.529	8.172
0.04	6.271	6.341	6.396	6.440	6.476
0.05	5.694	7.340	8.626	9.658	10.506
0.06	3.569	4.593	5.393	6.036	6.563
0.08	1.719	2.196	2.568	2.867	3.113
0.1	0.994	1.254	1.458	1.621	1.755
0.15	0.404	0.489	0.556	0.609	0.653
0.2	0.241	0.279	0.309	0.333	0.352
0.284	0.142	0.154	0.163	0.171	0.177
0.3	0.109	0.114	0.118	0.122	0.124
0.4	0.093	0.095	0.097	0.099	0.100
0.5	0.083	0.084	0.085	0.086	0.087

Energy (MeV)	Mass Attenuation Coefficient (cm^2/g)				
	S1	S2	S3	S4	S5
0.6	0.070	0.070	0.070	0.071	0.071
0.662	0.062	0.062	0.062	0.062	0.062
0.8	0.050	0.049	0.049	0.049	0.049
1	0.043	0.043	0.043	0.043	0.043
1.5	0.036	0.037	0.037	0.037	0.037
2	0.033	0.034	0.034	0.035	0.035
3	0.031	0.032	0.033	0.034	0.034
4	0.030	0.031	0.032	0.033	0.034
5	0.029	0.031	0.032	0.033	0.034
6	0.029	0.031	0.032	0.034	0.035
8	0.029	0.032	0.034	0.036	0.037

As photon energy rises from 15 keV to 15 MeV, the MAC experiences a rapid decrease initially (within 15 to 50 keV), then decreases more slowly, and ultimately stays constant. This decline in MAC is influenced by several factors namely, photoelectric effect (PE), compton scattering, (CS) and pair production, PP (Stalin et al., 2021).

MAC values rapidly decline at lower energies ($E \leq 0.5$ MeV) because of the photoelectric effect, which is proportional to and inversely related to energy raised to 3.5. In the intermediate energy band ($0.5 < E < 5$ MeV), Compton scattering takes precedence, varying as Z divided by E. For higher energies ($E > 5$ MeV), pair production dominates, with MAC values remaining almost unchanged for all samples (Sayyed et al., 2021).

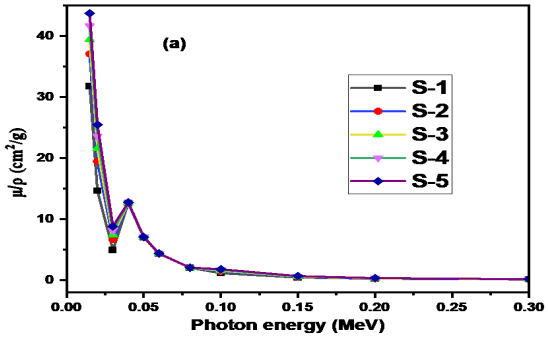

Figure 1: Variation of MAC of the glass samples with photon energy

The MAC of the glasses can be observed to increase as the Nd_2O_3 concentration of the sample increases as well, which could be due to the increase in density that correlates with Nd_2O_3 content. The results demonstrate MAC of the Nd^{3+} doped zinc tellurite glass system increase with varying concentration of Nd^{3+} in the order of S1 S2 S3 S4 S5. The MAC of the glasses decreases as energy increases because as the incoming radiation has more energy, more photons can penetrate through the sample, decreasing its absorption ability, and decreasing MAC. This trend also demonstrates that at lower energies the samples are the most effective, with S5 being the most, and as energy increases, their shielding ability becomes less effective, to the point that at high energies the differences between the shields are negligible. Nevertheless, at most energies, the S5 glass can be concluded to have superior attenuation abilities over the other investigated samples.

The MAC values of studied glasses are compared with those previous reported in radiation shielding glasses at the selected photon energy of 0.662 MeV as illustrated in the Fig. 2. It can be observed that the MAC value is higher than those reported in phosphate glass "ZBP-4" by, Borate glass "Sm 2.0" and commercial RS 253 glass, respectively. However, the result of MAC is comparable to that of SiO_2-MgO "SM1" glass material. The S-5 glass exhibits superb shielding efficacy due to its higher MAC compared to other investigated samples.

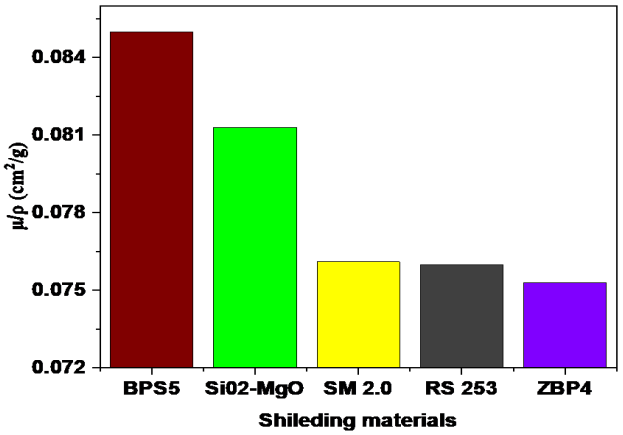

Figure 2: Comparison of MAC of the Studied Glass Sample with Previously Studied Shielding Materials

Linear Attenuation Coefficient (LAC)

The linear attenuation coefficient (LAC or μ) is a crucial parameter used in radiation shielding calculations to determine other shielding parameters like mean free path (MFP), half-value layer (HVL), and tenth-value layer (TVL) for the radiation absorber material. The attenuation of gamma-ray photons passing through an absorber is determined by different types of scattering and absorption processes. The linear attenuation coefficient (LAC or μ) depends on the energy and the density of the considered material. The LAC of the glass system under investigation rises alongside the Nd_2O_3 content. This is attributed to the gradual rise in density as the Nd_2O_3 content increases, as depicted in Figure 3 and Table 3. The values of LAC at the minimum incident photon energy (E = 0.015 MeV) are 100.707 (S1), 139.724 (S2), 171.811 (S3), 202.670 (S4) and 228.207 cm^{-1} (S5), respectively. Whereas, at the maximum energy (15 MeV), the LAC values were found to be 0.102 (S1), 0.122 (S2), 0.137 (S3), 0.152 (S4) and 0.158 cm^{-1} (S5) respectively.

Table 3: LAC Values Of the $[(Teo_2)_{0.70}(Zno)_{0.30}]_{(1-x)}$ $(Nd_2O_3$ Nps$)_{(X)}$, x = 0.01, 0.02, 0.03, 0.04, And 0.05 Mol Glass System Obtained Using Phy-X/PSD Software

Energy (MeV)	Linear Attenuation Coefficient (cm^2/g)				
	S1	S2	S3	S4	S5
1.50E-02	100.707	139.724	171.811	202.670	228.207
2.00E-02	46.640	64.847	79.827	94.229	106.151
3.00E-02	15.875	22.045	27.119	31.999	36.038
4.00E-02	22.012	24.223	25.711	27.368	28.557
5.00E-02	19.987	28.038	34.676	41.048	46.330
6.00E-02	12.526	17.545	21.681	25.653	28.945
8.00E-02	6.035	8.389	10.325	12.187	13.728
1 .00E-01	3.488	4.791	5.859	6.889	7.739
1.50E-01	1.419	1.869	2.234	2.588	2.879
2.00E-01	0.846	1.066	1.241	1.413	1.553
3.00E-01	0.498	0.588	0.656	0.726	0.780
4.00E-01	0.383	0.437	0.476	0.517	0.548
5.00E-01	0.326	0.364	0.391	0.420	0.442
6.00E-01	0.290	0.321	0.342	0.365	0.381
8.00E-01	0.245	0.268	0.283	0.300	0.312
1.00E+00	0.216	0.235	0.248	0.262	0.271
1.50E+00	0.174	0.189	0.198	0.209	0.216
2.00E+00	0.152	0.165	0.173	0.183	0.189
3.00E+00	0.128	0.140	0.149	0.158	0.165
4.00E+00	0.116	0.129	0.138	0.147	0.155

5.00E+00	0.109	0.123	0.132	0.143	0.150
6.00E+00	0.105	0.119	0.130	0.140	0.149
8.00E+00	0.101	0.117	0.128	0.140	0.150
1.00E+01	0.100	0.117	0.130	0.143	0.153
1.50E+01	0.102	0.122	0.137	0.152	0.164

Thus, the overall results of the LAC at both minimum and maximum photon energies show an increase as the content of Nd_2O_3 rises from 0.01 to 0.05 mol. eventually, the increase is slow in the compton and pair production absorption region. The increment of LAC implies that the sample containing a greater amount of neodymium oxide attenuates gamma photons much better compared with those containing less. This trend indicates a strong dependence of LAC on the atomic number of glass materials and the superiority of the S5 sample against radiation penetration. Previous studies have reported that rare earth element doped glasses improved shielding against gamma radiation.

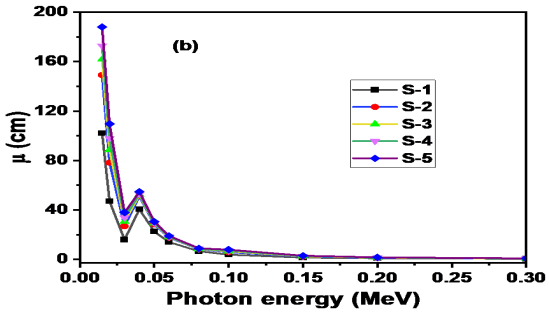

Figure 3: Variation of LAC of the Glass Samples with Photon Energy

Half Value Layer (HVL), Tenth Value Layer (TVL)

Half value layer (HVL) and Tenth value layer (TVL) are the thickness of the materials necessary to reduce the intensity of incident gamma photon by one half and one-tenth respectively. The lower the values of HVL and TVL, the higher the shielding against the gamma radiations. The HVL and TVL variations for Nd_2O_3 doped zinc tellurite glass system are shown in the Figures 4 and 5, respectively. At the lowest energy level, HVL values span from 0.057 cm in SBPS-1 to 0.024 cm in S-5. Similarly, TVL values decrease from 0.030 cm to 0.012 cm across the same samples. As photon energy rises from 0.015 MeV to 9 MeV, these values increase, but they start decreasing beyond 9 MeV. When Nd_2O_3 levels are raised from 0.01 mol% to 0.05 mol%, the values for both HVL and TVL drop, due to increased glass density from the high-Z Nd^{3+} ions. This leads to greater interactions between gamma photons and the material. Thus, S-1, with minimal Nd_2O_3, requires more thickness for radiation attenuation, while S-5 achieves the same with significantly less thickness. These findings highlight S-5's superior performance in gamma-ray shielding among the studied samples.

As reported previously, lower value of HVL means better shielding ability of the material. These evaluations concluded that the studied glasses show evidence of good shielding proficiency.

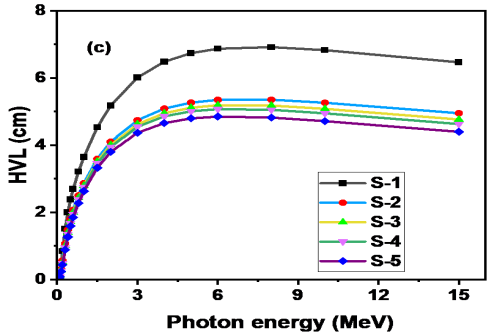

Figure 4: Variation of HVL of the Glass Samples with Photon Energy

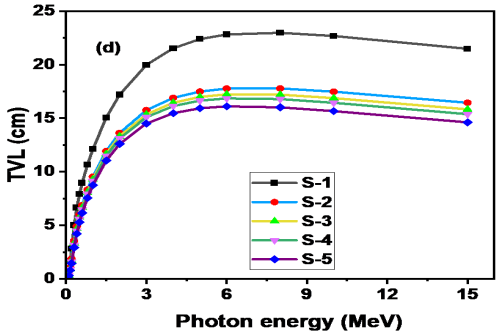

Figure 5: Variation of TVL of the Glass Samples with Photon Energy

Mean Free Path (MFP)

The mean free path (MFP) is another crucial metric for assessing the effectiveness of a material in shielding against gamma radiation. It defines the average distance a gamma photon covers between two interactions. Figure 6 and Table 4 present how MFP changes with photon energy in glasses with varying neodymium oxide content. Prior studies confirm that materials exhibiting lower MFP values generally offer better gamma-ray attenuation.

Table 4: MFP Values Of the $[(Teo_2)_{0.70}(Zno)_{0.30}]_{(1-x)}$ $(Nd_2O_3$ Nps$)_{(X)}$, x = 0.01, 0.02, 0.03, 0.04, And 0.05 Mol Glass System Obtained Using Phy-X/PSD Software

Energy (MeV)	Mean free path				
	S1	S2	S3	S4	S5
1.50E-02	0.010	0.007	0.006	0.005	0.004
2.00E-02	0.021	0.015	0.013	0.011	0.009
3.00E-02	0.063	0.045	0.037	0.031	0.028
4.00E-02	0.045	0.041	0.039	0.037	0.035
5.00E-02	0.050	0.036	0.029	0.024	0.022
6.00E-02	0.080	0.057	0.046	0.039	0.035
8.00E-02	0.166	0.119	0.097	0.082	0.073
1.00E-01	0.287	0.209	0.171	0.145	0.129
1.50E-01	0.705	0.535	0.448	0.386	0.347
2.00E-01	1.182	0.938	0.806	0.708	0.644
3.00E-01	2.009	1.702	1.524	1.378	1.282
4.00E-01	2.611	2.291	2.103	1.936	1.826
5.00E-01	3.071	2.746	2.556	2.378	2.262
6.00E-01	3.450	3.119	2.928	2.742	2.621
8.00E-01	4.080	3.732	3.533	3.332	3.203
1.00E+00	4.619	4.248	4.040	3.823	3.686
1.50E+00	5.740	5.300	5.055	4.796	4.633
2.00E+00	6.598	6.074	5.781	5.475	5.281
3.00E+00	7.827	7.126	6.724	6.324	6.066
4.00E+00	8.633	7.767	7.262	6.781	6.467
5.00E+00	9.165	8.154	7.561	7.016	6.657
6.00E+00	9.516	8.384	7.719	7.123	6.730
8.00E+00	9.872	8.559	7.790	7.127	6.688
1.00E+01	9.971	8.539	7.705	7.004	6.541
1.50E+01	9.799	8.221	7.315	6.583	6.101

At the lowest photon energy of 0.015 MeV, the MFP values are 0.010 cm for S-1 and 0.004 cm for S-5. At the higher energy level of 15 MeV, the MFP values rise to 9.799 cm and 6.101 cm for S5. These results indicate that glasses with higher neodymium oxide content and greater density exhibit lower MFP values, confirming their enhanced shielding performance against gamma radiation. According to the above trend, low incident photon energy might easily lose its energy in a few centimetres of penetration through Nd^{3+} doped zinc tellurite glass system compared to the high photon energy, which might penetrate a long distance before losing its energy.

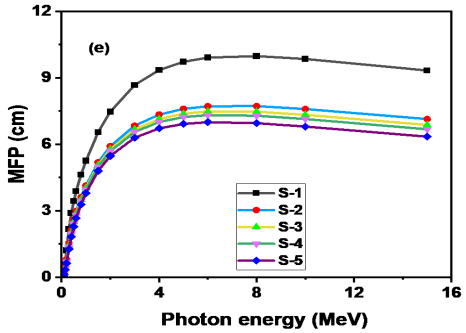

Figure 6: Variation of MFP of the Glass Samples with Photon Energy

Table 5: Mean Free Path (MFP) and Half Value Layer (HVL) Values of the Studied Glass and Some Other Shielding Materials at 662 Kev

Type of material	MFP (cm)	HVL (cm)
$(TeO_2)_{0.70}(ZnO)_{0.30}]_{(1-x)}(Nd_2O_3\ NPs)_{(x)}$, (present)	2.812	1.782
Concrete (Kumar, 2017)	5.5803	3.867
30BiBTe glass (Halimah et al., 2019)	2.9265	2.0281
50BaO–xBi2O3–(50–x) borosilicate glass (Bagheri et al., 2017)	1.7215	1.1929

A comparative analysis was conducted at 662 keV to establish the validity of the present study in term of HVL and MFP of materials in the other studies. The HVL and MFP values for S-S glasses of the present work are lower than that obtained in the previous studies by for concretes (Kumar, 2017) and for 30BiBTe glass (Halimah et al., 2019). However, HVL and MFP values are comparable to those obtained for Barium borosilicate glass (Bagheri et al., 2017), as shown in Table 5. It can be concluded that S5 glass has better attenuation ability, surpassing other samples investigated. In Table 5, we compare the MFP values of the current glass systems with Nd^{3+} doped systems at some specified photon energies. Notably, there is good evidence that the current glass systems under study can actively act as gamma ray shielding materials.

CONCLUSION

The main goal of the current study was to evaluate the effect of rare earth (Nd^{+3}) on gamma photon shielding properties of Nd^{3+} doped zinc tellurite glass. The chemical forms of the glass system are $[(TeO_2)_{0.70}(ZnO)_{0.30}]_{(1-x)}(Nd_2O_3\ NPs)_{(x)}$, x = 0.01, 0.02, 0.03,0.04, and 0.05 mol glass system with sampling code S-1, S-2, S-3, S-4 and S-5, respectively. The gamma photon shielding parameters were evaluated at energy range of 0.015 and 15 MeV, the results revealed that the values of MAC and LAC increased as the Nd_2O_3 concentration and density of the glass samples increased. The MAC values are higher at the lower photon energy of 15 KeV, increasing from 28.691 cm²/g to 51.748 cm²/g as the Nd_2O_3 concentration increases from 0.01 to 0.05 mol. The progressive rise in MAC from samples S1 to S5 suggests a dependence on the Nd_2O_3 content, or oxide ion concentration, possibly due to substituting heavier Nd_2O_3 molecules with lighter TeO_2 molecules in the glass system. The values of LAC at the minimum incident photon energy (E = 0.015 MeV) are 100.707 (S1), 139.724 (S2), 171.811 (S3), 202.670 (S4) and 228.207 cm^{-1} (S5), respectively. Whereas, at the maximum energy (15 MeV), the LAC values were found to be 0.102 (S1), 0.122 (S2), 0.137 (S3), 0.152 (S4) and 0.158 cm^{-1} (S5) respectively.

At the lowest energy level, HVL values span from 0.057 cm in SBPS-1 to 0.024 cm in S-5. Similarly, TVL values decrease from 0.030 cm to 0.012 cm across the same samples. As photon energy rises from 0.015 MeV to 9 MeV, these values increase, but they start decreasing beyond 9 MeV. When Nd_2O_3 levels are raised from 0.01 mol% to 0.05 mol%, the values for both HVL and TVL drop, due to increased glass density from the high-Z Nd^{3+} ions. This leads to greater interactions between gamma photons and the material. Thus, S-1, with minimal Nd_2O_3, requires more thickness for radiation attenuation, while S-5 achieves the same with significantly less thickness. These findings highlight S-5's superior performance in gamma-ray shielding among the studied samples.

REFERENCES

Alomari, A. H., 2024. Enhancing radiation shielding effectiveness: a comparative study of barium-doped tellurite glasses for gamma and neutron radiation protection. Journal of Taibah University for Science, 8(1), p. 2328370.

Alomari, A. H., 2024. Enhancing radiation shielding effectiveness: a comparative study of barium-doped tellurite glasses for gamma and neutron radiation protection. Journal of Taibah University for Science, 8(1), p. 2328370.

Dong, M.; Zhou, S.; Xue, X.; Feng, X.; Sayyed, M.I.; Khandaker, M.U.; Bradley, D.A. The potential use of boron containing resources for protection against nuclear radiation. Radiat. Phys. Chem. 2021, 188, 109601.

P. Vani, G. Vinitha, M. I. Sayyed, M. M. AlShammari and. N. Manikandan, "Effect of rare earth dopants on the radiation shielding properties of barium tellurite glasses." Nuclear Engineering and Technology, vol. 53(12), pp. 4106-4113, 2021.

I. G. Geidam, K. A. Matori, M. K. Halimah, K. T. Chan, F. D. Muhammad, M. Ishak and S. A. Umar, "Oxide ion polarizabilities and gamma radiation shielding features of TeO2–B2O3–SiO2 glasses containing Bi2O3 using Phy-X/PSD software," Materials Today Communications, vol. 31, p. 103472, 2022.

Rammah, Y.S., Mahmoud, K.A., Sadeq, M.S., Haily, E., Bih, L., Ahmed, E.M. and El-Agawany, F.I., 2022. Optical and radiation shielding properties of titano-phosphate glasses: influence of BaO. Journal of the Australian Ceramic Society, 58(3), pp.867-880.

M. I. Sayyed, A. Saleh, A. Kumar and F. E. Mansour, "Experimental examination on physical and radiation shielding features of boro-silicate glasses doped with varying amounts of BaO," Nuclear Engineering and Technology, 2024.

M. K. Halimah, A. Azuraida, M. Ishak and L. Hasnimulyati, "Influence of bismuth oxide on gamma radiation shielding properties of boro-tellurite glass. Journal of non-crystalline solids," 512, pp. 140-147, 2019.

U.S. Aliyu, H.M. Kamari, I.G. Geidam, I.O. Alade, A.M. Noorazlan, A.M. Hamza, A. F. Ahmad, Spectroscopic investigations of Er2O3 doped silica borotellurite glasses, Opt. Mater. 114 (2021), 110987, https://doi.org/10.1016/j.optmat.2021.110987.

H. M. Zakaly, S. Y. Rammah, H. O. Tekin, A. Ene, A. Badawi and S. A. Issa, "Nuclear shielding performances of borate/sodium/potassium glasses doped with Sm3+ ions. Journal of materials research and technology," journal of materials research and technology, 18, pp. 1424-1435, 2022.

Lotfi-Omran, O.; Sadrmomtazi, A.; Nikbin, I.M. A comprehensive study on the effect of water to cement ratio on the mechanical and radiation shielding properties of heavyweight concrete. Construct. Build. Mater. 2019, 229, 116905.

Holynska, B. Study of the effect of grain size heterogeneity in the X-ray absorption analysis of simulated aqueous slurries. Spectrochim. Acta 27, 237 (1972).

N. J. AbuAlRoos, N. A. B. Amin and R. Zainon, "Conventional and new lead-free radiation shielding materials for radiation protection in nuclear medicine: A review," Radiation Physics and Chemistry, vol. 165, p. 108439, 2019.

A. H. Alomari, "Enhancing radiation shielding effectiveness: a comparative study of barium-doped tellurite glasses for gamma and neutron radiation protection," Journal of Taibah University for Science. 8, no. 1, p. 2328370, 2024.

Singh, V.P., Badiger, N.M., Kaewkhao, J., 2014b. Radiation shielding competence of silicate and borate heavy metal oxide glasses: comparative study. J. Non-Cryst. Solids 404 (11), 167–173. https://doi.org/10.1016/j.jnoncrysol.2014.08.003 Elsevier B.V.

Effects of environmental lead exposure on T-helper cellspecific cytokines in children. J. Immunotoxicol. 8 (10), 284–287. https://doi.org/10.3109/1547691X.2011.592162.

The heavy metal oxide glasses within the WO 3 -MoO 3 -TeO 2 system to investigate the shielding properties of radiation applications. Prog. Nucl. Energy 104 (9), 280–287. https://doi.org/10.1016/j.pnucene.2017.10.008.

J. A. Jiménez and M. Sendova, "UV-sensitized Sm3+ visible and near-IR photoluminescence in phosphate glass melted with multi-wall carbon nanotubes." Journal of Non-Crystalline Solids 498, pp. 455-460, 2018.

K. A. Naseer, K. Marimuthu, N. Almousa and M. I. Sayyed, "Investigations on physical, structural, elastic, optical and radiation shielding properties of calcium phospho-silicate glasses," Radiation Physics and Chemistry, 214, p. 111306, 2024.

M. G. Dong, R. El-Mallawany, M. I. Sayyed and M. O. Tekin, "Shielding properties of 80TeO2–5TiO2–(15− x) WO3–xAnOm glasses using WinXCom and MCNP5 code." Radiation Physics and Chemistry. 141, pp. 172-178, 2017.

M. I. Sayyed, B. O. Elbashir, H. O. Tekin, E. E. Altunsoy and D. K. Gaikwad, "Radiation shielding properties of pentaternary borate glasses using MCNPX code." Journal of Physics and Chemistry of Solids, 121, pp. 17-21, 2018.

Y. S. Itas, M. D. Albaqami, S. Mohammad, M. U. Khandaker, M. R. Mohammad. R. Haldhar and M. K. Hossain, "Investigation on radiation shielding potentials of barium calcium aluminosilicate glass material using silicon carbide nanotubes reinforcement," Radiation Physics and Chemistry. 225, p. 112158, 2024.

E. Şakar, Ö. F. Özpolat, B. Alım, M. I. Sayyed and M. Kurudirek, "development of a user friendly online software for calculation of parameters relevant to radiation shielding and dosimetry.," Radiation Physics and Chemistry. 166, p. 108496, 2020.

M. I. Sayyed, B. O. Elbashir, H. O. Tekin, E. E. Altunsoy and D. K. Gaikwad, "Radiation shielding properties of pentaternary borate glasses using MCNPX code." Journal of Physics and Chemistry of Solids, vol. 121, pp. 17-21, 2018.

Sayyed, M. I. et al., 2020. Evaluation of gamma-ray and neutron shielding features of heavy metals doped Bi2O3-BaO-Na2O-MgO-B2O3 glass systems. Progress in Nuclear Energy, Volume 118, p. 103118.

Singh, G. P., Singh, J., Kaur, P., Kaur, S., Arora, D., Kaur, R., Kaur, K. & Singh, D. 2020. Analysis Of Enhancement In Gamma Ray Shielding Proficiency By Adding Wo3 In Al2o3-Pbo-B2o3 Glasses Using Phy-X/Psd. Journal Of Materials Research And Technology, 9, 14425-14442.

Stalin, S., Gaikwad, D.K., Al-Buriahi, M.S., Srinivasu, C., Ahmed, S.A., Tekin, H.O., Rahman, S., 2021. Influence of Bi2O3/WO3 substitution on the optical, mechanical, chemical durability and gamma ray shielding properties of lithium-borate glasses. Ceram. Int. 47 (4), 5286–5299

Tijani SA, Kamal SM, Al-Hadeethi Y, Arib M, Hussein MA, Wageh S, et al. Radiation shielding properties of transparent erbium zinc tellurite glass system determined at medical diagnostic energies. J Alloys Compd 2018; 741:293–9. https://doi.org/10.1016/j.jallcom.2018.01.109.

Singh VP, Badiger NM, Chanthima N, Kaewkhao J. Evaluation of gamma-ray exposure buildup factors and neutron shielding for bismuth borosilicate glasses. Radiat Phys Chem 2014; 98:14–21. https://10.1016/j.radphyschem.2013.12.029.

Kirdsiri K, Kaewkhao J, Chanthima N, Limsuwan P. Comparative study of silicate glasses containing Bi2O3, PbO and BaO: Radiation shielding and optical properties. Ann Nucl Energy 2011; 38:1438–41. https://doi.org/10.1016/j.anucene.2011.01.031.

Ruengsri S, Insiripong S, Sangwaranatee N, Kaewkhao J. Development of barium borosilicate glasses for radiation shielding materials using rice husk ash as a silica source. Prog Nucl Energy 2015; 83:99–104. https://doi.org/10.1016/j.pnucene.2015.03.006.

El-Mallawany R, Sayyed MI, Dong MG. Comparative shielding properties of some tellurite glasses: Part 2. J Non Cryst Solids 2017; 474:16–23. https://doi.org/10.1016/j.jnoncrysol.2017.08.011

Halimah, M. K., et al. "Effect of neodymium nanoparticles on optical properties of zinc tellurite glass system." Journal of Materials Science: Materials in Electronics 31 (2020): 3785-3794.

Trubey MJH, Berger DK. Photon cross sections for endf/b-vi*; 2008.

Zakaly, H. M. et al., 2022. Nuclear shielding performances of borate/sodium/potassium glasses doped with Sm3+ ions. Journal of materials research and technology. Journal of materials research and technology, Volume 18, pp. 1424-1435.